

Role of placenta growth factor in malignancy and evidence that an antagonistic PIGF/Flt-1 peptide inhibits the growth and metastasis of human breast cancer xenografts

Alice P. Taylor and David M. Goldenberg

Garden State Cancer Center, Center for Molecular Medicine and Immunology, Belleville, New Jersey

Abstract

The angiogenic growth factor, placenta growth factor (PIGF), is implicated in several pathologic processes, including the growth and spread of cancer. We found by immunohistochemistry that 36% to 60% and 65% of primary breast cancers express PIGF and its receptor Flt-1, respectively. These findings suggest that PIGF may be active in tumor growth and metastasis beyond its role in angiogenesis. It was found that exogenously added PIGF (2 nmol/L), in contrast to vascular endothelial growth factor (2 nmol/L), significantly stimulated *in vitro* motility and invasion of the human breast tumor lines MCF-7 and MDA-MB-231. A PIGF-2/Flt-1-inhibiting peptide, binding peptide 1 (BP1), that binds Flt-1 at or near the heparin-binding site was identified and synthesized. Both PIGF-stimulated motility and invasion were prevented by treatment with BP1 ($P < 0.05$), as well as by anti-PIGF antibody. Treatment of mice bearing s.c. MDA-MB-231 with BP1 (200 μ g i.p., twice per week) decreased the number of spontaneous metastatic lung nodules by 94% ($P < 0.02$), whereas therapy of animals with orthotopic mammary fat pad tumors decreased pulmonary metastases by 82% ($P < 0.02$). These results indicate, for the first time, that PIGF stimulates the metastatic phenotype in these breast cancer cells, whereas therapy with a PIGF-2/Flt-1 heparin-blocking peptide reduces the growth and metastasis of human breast cancer xenografts. [Mol Cancer Ther 2007;6(2):524–31]

Introduction

Placenta growth factor (PIGF), a member of the vascular endothelial growth factor (VEGF) family, participates

actively in the angiogenesis of diverse cancers (1–5). First cloned from placenta (6), PIGF is normally expressed by trophoblasts, by normal thyroid, and during wound healing (7, 8). In trophoblasts, expression of PIGF is abrogated by hypoxic stress (9), but hypoxia-driven expression has been found in at least one primary tumor (10), in tumor xenografts (11), and in fibroblasts (12). In addition, many malignancies express the PIGF receptor Flt-1 (13).

The more studied isoform of PIGF, PIGF-2, includes a 21-amino acid heparin-binding domain and binds both of the known PIGF receptors neuropilin-1 (NRP-1) and Flt-1. PIGF-1, which lacks the heparin-binding domain, binds only Flt-1 (14, 15). Flt-1 is a member of the tyrosine kinase family of receptors (receptor tyrosine kinase), whereas NRP-1 is not, and most likely associates with receptor tyrosine kinases for activity (16). The second Flt-1 extracellular domain interacts with PIGF, but its fourth domain contains a heparin-binding region that potentially brings Flt-1 and its ligand into closer association (17). As with other receptor tyrosine kinase–ligand pairs, the heparin-binding domains of PIGF and Flt-1 may be essential for full activation of the receptor (18, 19). When bound to Flt-1, PIGF-2 is capable of inducing differentiation, proliferation, and migration of endothelial cells (20).

In our investigation of tumor recurrence, we detected PIGF production by surviving tumor cells after treatment with radiolabeled antibodies (11, 21) even when PIGF was undetectable before treatment. PIGF is a known survival factor for endothelial cells (22), but its treatment-induced expression by tumor cells was unexpected. Further investigation correlated PIGF expression with enhanced recovery from cytotoxic treatment (21). These findings suggest that PIGF affects tumor cells and the tumor environment. Therefore, this study investigates the role of PIGF in cancer growth and metastasis focused on breast cancer.

Materials and Methods

Isolation of Phage

A phage library (Ph.D.-12 Phage Display Peptide Library kit, New England Biolabs, Inc., Ipswich, MA) was panned on recombinant human PIGF-2 or recombinant human VEGF165 (R&D Systems, Flanders, NJ) according to the suppliers' methods. Subsequent panning was done using either PIGF or a peptide corresponding to the putative receptor-binding site on the PIGF molecule. Phage were submitted to three rounds of panning and plated out on agar in a series of 10-fold dilutions for titers. Well-isolated plaques were picked from the titer plates and amplified for further investigation.

Received 8/2/06; revised 11/6/06; accepted 12/13/06.

Grant support: Breast Cancer Concept award DAMD17-03-1-0758 from the U.S. Department of Defense (A.P. Taylor) and New Jersey Department of Health and Senior Services grant 05-1842-FS-N-0 (D.M. Goldenberg).

The costs of publication of this article were defrayed in part by the payment of page charges. This article must therefore be hereby marked *advertisement* in accordance with 18 U.S.C. Section 1734 solely to indicate this fact.

Requests for reprints: Alice P. Taylor, Garden State Cancer Center, Center for Molecular Medicine and Immunology, 520 Belleville Avenue, Belleville, NJ 07109. Phone: 973-844-7009; Fax: 973-844-7020. E-mail: ataylor@gscancer.org

Copyright © 2007 American Association for Cancer Research.

doi:10.1158/1535-7163.MCT-06-0461

Sequencing

DNA was isolated from amplified plaques and sequenced using the primer suggested by the Ph.D. kit (M13 phage-specific), and the Thermo Sequenase Radio-labeled Terminator Cycle Sequencing kit (U.S. Biochemical, Swampscott, MA). Binding peptide 1 (BP1) contains 20 amino acids. A control peptide, CPA, was derived by substituting A for the H, R, and D residues in BP1. BP1 and CPA were synthesized commercially (University of Georgia) and investigated *in vitro* and *in vivo*.

Testing of Free Peptide Binding to PIGF, VEGF, or Flt-1

The protocol suggested by the supplier of the phage display system for panning was followed. Free peptide binding was determined by coating 96-well plates with PIGF (10 $\mu\text{g}/\text{mL}$), recombinant human Flt-1 fusion protein (10 $\mu\text{g}/\text{mL}$; R&D Systems), or VEGF (10 $\mu\text{g}/\text{mL}$). Competition assays were done with 2.5 or 25 units/mL heparin (Sigma, St. Louis, MO). The peptides used in these experiments contained a linker and the FLAG epitope at the COOH terminus (DYKDDDDK). Thirty minutes after the addition of the first reagent, the second reagent was added followed by incubation for another 30 min together. Peptide binding was assessed by probing for the FLAG epitope (23, 24). Absorbance was read at 490 nm. In ELISA-based binding assays, CPA bound PIGF and VEGF but showed attenuated affinity (50%) for Flt-1. The CPA peptide was consistently inactive *in vitro* and *in vivo*.

Flow Cytometry, Immunohistochemistry, and Histopathology

Antibodies to PIGF and VEGF used in this study were tested for cross-reactivity by ELISA and immunoblot. No cross-reactivity was detected. Antibodies were also tested for inhibition of the target growth factor in angiogenesis assays; both antibodies showed 20% to 80% inhibition of angiogenesis when their target growth factor was added.

Flow cytometry was done by standard methods using 1 to 5 $\mu\text{g}/\text{mL}$ of primary antibody and 1:500 dilution of FITC-labeled secondary antibody (Biosource International, Camarillo, CA). Data were collected on a BD FACSCalibur flow cytometer (BD Biosciences, Rockville, MD) using Cell Quest software.

Paraffin-embedded primary breast cancer tissue arrays from two sources (US Biomax, Inc., Rockville, MD, and Tissue Array Research Program, National Cancer Institute, Bethesda, MD) were stained using standard immunohistochemistry procedures (11) for PIGF and VEGF expressions. Tissue arrays were also probed for Flt-1 or NRP-1 (ABXIS, Seoul, Korea). Antibodies were purchased from Santa Cruz Biotechnology, Inc. (Santa Cruz, CA). Stained slides were examined at $\times 100$ and rated by assigning relative values that reflected the intensity of staining: faint ($0.25 < 0.5$), moderate ($0.5 < 1.0$), heavy ($1.0 < 2.0$), and intense (> 2.0); scoring was in 0.25-point increments. Only viable-appearing areas of tumor epithelium and endothelium were assessed, and a value representing the overall intensity and percentage of cells that were stained was assigned to each slide or tissue section. Staining of extracellular connective

tissues and WBC was not included. Background staining with an irrelevant antibody, Ag8, was subtracted. Tumor specimens were considered positive if staining intensity was ≥ 0.5 . Human tumor xenograft samples were also stained with H&E by standard methods.

Cell Lines

To further characterize the cell lines used in this report, MCF-7, MDA-MB-231, and MDA-MB-468 (American Type Culture Collection, Manassas, VA) were assayed for PIGF or VEGF expression by flow cytometry (Supplementary Fig. S1A and B shows selected tissue section).¹ MDA-MB-231, MDA-MB-468, and MCF-7 were also tested for expression of the estradiol receptor α (Santa Cruz Biotechnology) by immunohistochemistry of cell monolayers. MCF-7 was positive and MDA-MB-231 and MDA-MB-468 were negative for estrogen receptor. MDA-MB-231 and MDA-MB-468 xenograft tumors were also probed for Flt-1 by immunohistochemistry and were positive (Supplementary Fig. S1C).¹ No MCF-7 tumors were available, but immunohistochemical staining of tissue culture grown cells indicated the presence of Flt-1 (not shown).

Cell Migration and Invasion Assays

PIGF and VEGF were tested for activity with human endothelial cells and were both capable of inducing spontaneous migration (VEGF, 3.5-fold; PIGF, 2-fold). MCF-7, MDA-MB-231, and MDA-MB-468 or endothelial cells were cultured on sterile glass coverslips. The monolayers were scratched ("wounded") with a plastic pipette tip, and, after washing, treated alone or in combination with PIGF or VEGF (2 nmol/L), peptides (2 $\mu\text{mol}/\text{L}$), or with antibody (0.67–1 $\mu\text{g}/\text{mL}$; refs. 25–27). Inhibitor concentration consisted of human recombinant soluble Flt-1 (R&D Systems) at 2 nmol/L. Peptides or soluble Flt-1 was incubated with PIGF-containing or VEGF-containing medium for 10 min before addition to cells. Stained (Wright-Giemsa) and mounted coverslips were examined microscopically. Five to ten $\times 100$ fields were evaluated by counting the number of cells separated from the wound edges and which seemed to be migrating toward the center of the wound. Results are reported as the average number of cells migrating into the wound per $\times 100$ field. In some cases, data from separate experiments were combined to accommodate inclusion of various treatments in the tables.

Cellular invasion was determined by addition of 5×10^4 cells to growth factor-reduced Matrigel invasion chambers (BD Biosciences Discovery Labware, Bedford, MA) according to the protocol provided by the supplier. Growth factors (2.0 or 0.2 nmol/L), peptide (2 $\mu\text{g}/\text{mL}$), or antibody (1 $\mu\text{g}/\text{mL}$) was added to cells in low-serum [0.1% fetal bovine serum (FBS)] medium. Baseline (0.1% serum, no added growth factor or peptides) and chemoattractant-based invasions (10% FBS in bottom chamber) were included. The number of invading cells was determined

¹ Supplementary material for this article are available at Molecular Cancer Therapeutics Online (<http://mct.aacrjournals.org/>).

by counting the number of cells on the bottom of the invasion chamber membrane after staining at $\times 100$ after 24 h (MDA-MB-231) or 48 h (MCF-7 and MDA-MB-468). The results of three to five separate experiments are presented.

Treatment with Peptides *In vivo*

In s.c. tumor model, the tissue culture-grown human breast tumor cell line MDA-MB-231 was implanted s.c. on the flanks of nude mice in two experiments (10^7 cells, $n = 4-5$ mice per treatment per experiment). When tumors were measurable, the mice were redistributed so that small, medium, and large tumors were evenly distributed among the treatment groups; cages were randomly assigned treatments. The mice were weighed, and the volume of tumors was calculated by multiplying the caliper-measured length \times width \times depth. Orthotopic tumors were not measured in this fashion, but the tumors were weighed at the end of the experiment, and the weight was expressed in grams per tumor. Treatment with peptides was begun on day 28 and day 20 after implantation in s.c. experiments 1 and 2, respectively. Mice were treated with 200- μ g peptide in PBS by i.p. injection at 3-day to 4-day intervals for 4 weeks (experiment 1, nine doses; experiment 2 and the orthotopic experiment, eight doses). Durations of treatment were 30 days for experiment 1 (s.c.) and 27 to 28 days for experiment 2 (s.c.) and the orthotopic experiment. Animals were weighed, and tumors were measured at each treatment (s.c.). Seven days after the final treatment (8.5 weeks after implantation), tumors and lungs were harvested from experiment 1. In experiment 1, tumor size averages (in volume) at the beginning of treatment were $128 \pm 54 \text{ mm}^3$ (range, 70–183 mm^3) for the mock-treated group and $106 \pm 57 \text{ mm}^3$ (range, 50–180 mm^3) for the BP1-treated group; tumor sizes at the last treatment were $689 \pm 559 \text{ mm}^3$ (range, 255–1,319 mm^3) for the mock-treated group and $448 \pm 308 \text{ mm}^3$ (range, 35–770 mm^3) for the BP1-treated group. In experiment 2, tumor sizes at the beginning of treatment were $75 \pm 55 \text{ mm}^3$ (range, 38–170 mm^3) for the mock-treated group, $57 \pm 46 \text{ mm}^3$ (range, 21–131 mm^3) for the CPA-treated group, and $81 \pm 87 \text{ mm}^3$ (range, 20–232 mm^3) for the BP1-treated group; tumor sizes at the last treatment were $418 \pm 183 \text{ mm}^3$ (range, 263–620 mm^3) for the mock-treated group, $332 \pm 271 \text{ mm}^3$ (range, 56–638 mm^3) for the CPA-treated group, and $56 \pm 23 \text{ mm}^3$ (range, 34–85 mm^3) for the BP1-treated group. Tumor burden of the lungs was determined (experiment 1) by counting colonies (<20 cells), clusters (>20–100 cells), and nodules (>100 cells) seen in all the lung tissues on a total of four slides, two lung sections per slide, for each mouse. Data are presented as the average number of each size of metastasis for each treatment group (three to four mice per group). The total number of each was summed for each treatment group and divided by the total number of mice in that group. The percentage inhibition for metastasis was determined by the formula: percentage inhibition = (number of mock-treated metastases – number of treated metastases / number of mock-treated metastases) \times 100. Experiment 2 was terminated 3 days after the last treatment. Lungs from experiment 2 were not evaluated.

In experiment 2, mice were treated with a control peptide, CPA, for which *in vitro* data are also presented. Dosage, timing, and duration of treatment were based on experience with another xenograft tumor line (not shown).

MDA-MB-231 was also implanted in the mammary fat pad of SCID mice (3×10^6 cells, five mice per treatment). SCID mice were chosen because this strain is often used for orthotopic implantation of xenografts that metastasize (28). In this model, large pulmonary metastases were not observed, perhaps because of the early time point chosen for the initiation of treatment. Peptide treatment was commenced on day 5 after implantation, when tumors were palpable in all mice. Treatment schedule and dose were as described above (eight treatments). Measurement of the volume of orthotopic tumors is not reliable, and so 3 days after the final peptide treatment, which was ~ 5 weeks after implantation, the tumors were removed and weighed. Lungs were harvested and examined microscopically for metastases, as described above.

Guidelines set by Center for Molecular Medicine and Immunology Research Animal Resource Center were followed in these experiments.

Statistical Analyses

Statistical analysis of binding, viability, motility, angiogenesis, tumor growth, and metastatic tumor burden were evaluated by ANOVA. $P < 0.05$ was considered significant.

Results

The frequency of constitutive PIGF and PIGF-receptor expression by primary breast cancer and breast tumor cell lines was investigated by immunohistochemical staining of tissue arrays (see Materials and Methods). Results are shown in Table 1 and Supplementary Fig. S1A and B.¹ This analysis showed a higher proportion of samples positive for PIGF than VEGF (PIGF, 43–60%; VEGF, 13–14%). Expression of the PIGF receptor, NRP-1, was limited to breast cancer parenchyma (27%) but not tumor endothelium. On the other hand, both tumor parenchyma and endothelium were positive for Flt-1 (65% and 56%, respectively).

Human breast cancer cell lines, MCF-7, MDA-MB-231, and MDA-MB-468, were analyzed for PIGF and VEGF

Table 1. Expression of PIGF, VEGF, NRP-1, and Flt-1 by primary breast cancers

Marker	Array 1 (%)	Array 2 (%)
PIGF	30/69 (43%)	30/50 (60%)
VEGF	9/70 (13%)	7/50 (14%)
NRP-1	ND	25/94 (27%)
Flt-1 tumor	ND	31/48 (65%)
Flt-1 vessels	ND	27/48 (56%)

NOTE: Number of moderate to strong staining tumors per total number of samples per array [Array 1, from Tissue Array Research Program; Array 2, commercial source (see Materials and Methods)].

Abbreviation: ND, not done.

expression by flow cytometry. The percentages of PIGF-positive cells were 29%, 49%, and 38% for MCF-7, MDA-MB-231, and MDA-MB-468, respectively. The percentages of VEGF-positive cells were 8%, 18%, and 13% for MCF-7, MDA-MB-231, and MDA-MB-468, respectively (Supplementary Fig. S1D).¹ Thus, these cell lines were relatively high expressers of PIGF and low expressers of VEGF. Both MDA-MB-231 and MDA-MB-468 xenograft tumors and tissue culture-grown MCF-7 express the PIGF receptor Flt-1 (MCF-7 not shown; Supplementary Fig. S1C).¹ MDA-MB-468 stained faintly for NRP-1 (not shown), and NRP-1 expression by MDA-MB-231 has already been documented (19). These cell lines were used for subsequent investigation.

The relatively high frequency of PIGF, NRP-1, and Flt-1 expressions by breast cancer cells suggested that PIGF may have a direct effect on these cells. To investigate the effects of PIGF on breast cancer cells, PIGF and Flt-1 were obtained by panning of a phage peptide library. After isolation, phages were subjected to an ELISA-based binding assay on PIGF-coated plates. The absorbance readings (410 nm) for the phage BP1, the peptide which is reported here, was 0.024 (Phage library background 0.003).

Free peptide, BP1 (SHRYRLAIQLHASDSSSSCV), was synthesized with a C-terminal FLAG epitope and tested for binding to PIGF, Flt-1, and VEGF. We found that BP1 bound to PIGF (A490, 0.100 ± 0.058) and VEGF165 (A490, 0.299 ± 0.174) but most strongly to Flt-1 (A490, 0.886 ± 0.096). Flt-1 binding was further tested by the addition of unbound Flt-1 to binding assays; addition of free Flt-1 (2 nmol/L) caused a 38% decrease in binding of BP1 to immobilized Flt-1 (A490 for 5 $\mu\text{mol/L}$ BP1 only, 0.527 ± 0.025 ; with added free Flt-1 and BP1, 0.327 ± 0.127).

Additional assays were done to determine if the presence of PIGF would interfere with the BP1-Flt-1 interaction. PIGF at concentrations between 1 and 100 nmol/L had no significant effect on the binding of BP1 to Flt-1. These findings suggested that BP1 interacted with a site on Flt-1 other than domain 2, where the major interactions of PIGF with Flt-1 are located. Subsequently, the association of BP1 with the heparin-binding sites present on both Flt-1 and PIGF-2 was investigated. As shown in Fig. 1, addition of heparin to Flt-1-coated plates before addition of BP1 resulted in a 64% decrease in BP1 binding ($P < 0.0002$). However, when BP1 was added before the addition of heparin, the binding of BP1 was inhibited by only 13% ($P > 0.05$). Thus, BP1 most likely binds to Flt-1 at or near the heparin-binding site.

Next, we asked whether PIGF could increase the likelihood of tumor recurrence or metastasis. Because metastatic tumor cells display increased motility and invasive potential, exogenous PIGF was added to motility and invasion assays containing the breast cancer cell lines MCF-7, MDA-MB-231, and MDA-MB-468. PIGF caused a 1.8-fold to 2.1-fold increase in motility of MDA-MB-231 and MCF-7 ($P < 0.01$) but did not significantly affect the motility of MDA-MB-468. Addition of recombinant soluble Flt-1 (2 nmol/L) significantly blocked the stimulatory effect of

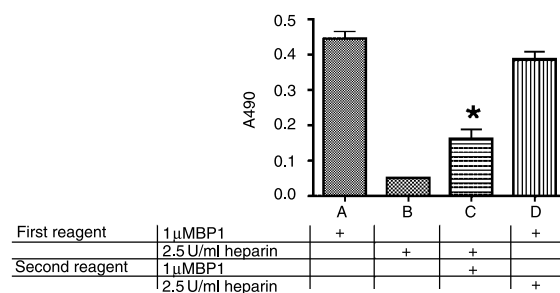


Figure 1. BP1 interacts with the heparin-binding region of Flt-1. Reagents were added to Flt-1-coated wells as indicated in the table below the figure. **A**, 1 $\mu\text{mol/L}$ BP1 only; **B**, 2.5/25 units/mL heparin only; **C**, 2.5 units/mL heparin followed by 1 $\mu\text{mol/L}$ BP1; **D**, 1 $\mu\text{mol/L}$ BP1 followed by 2.5 units/mL heparin. Columns, mean of duplicate wells ($n = 2$ experiments); bars, SD. *, $P < 0.0002$ for heparin followed by 1 $\mu\text{mol/L}$ BP1 (C) versus BP1 only (A; ANOVA).

PIGF by 55% and 67% for MDA-MB-231 and MCF-7, respectively ($P < 0.02$; Table 2). Anti-PIGF antibody (1 $\mu\text{g/mL}$) also blocked the PIGF-mediated motility of MDA-MB-231 and MCF-7 ($P < 0.02$; Table 2). BP1 also inhibited PIGF-stimulated motility in MDA-MB-231 and MCF-7 significantly ($P < 0.02$). Control antibody (Ag8) and peptide, CPA, had no effect, nor did VEGF (2 nmol/L; Table 2). Anti-VEGF antibody added to PIGF-containing assays did not affect PIGF-stimulated migration of MDA-MB-231, suggesting that the increased motility observed in this cell line was not due to VEGF activity (Table 2).

Although exogenously added PIGF did not significantly increase motility in MDA-MB-468, addition of soluble Flt-1 or anti-PIGF to PIGF-containing MDA-MB-468 cultures significantly inhibited its motility ($P < 0.05$; Table 2). The inhibitory effect of Flt-1 and anti-PIGF on MDA-MB-468 suggests the presence of PIGF in the tissue culture medium, whether from the FBS or from PIGF produced by the cells. The effects of Flt-1 and anti-PIGF also suggest that the motility of this cell line is maximal without added PIGF and that more PIGF will not stimulate further motility. Also, addition of BP1 alone (2 $\mu\text{mol/L}$) to MDA-MB-468, without PIGF, inhibited motility [11.4 ± 8.5 (untreated) versus 6.9 ± 4.4 (BP1 only) migrating cells per $\times 100$ field; $P < 0.001$], further suggesting that PIGF is present in the culture and that it influences the motility of this cell line.

Because the ability to invade the basement membrane is essential for metastasis, invasion assays with added PIGF or VEGF were done. Addition of PIGF at both 2.0 and 0.2 nmol/L resulted in nearly 3-fold increased invasion of MDA-MB-231 after 24 h [11 ± 8.1 (untreated) versus 30 ± 13.7 (2.0 nmol/L PIGF treated) or 28 ± 12 (0.2 nmol/L PIGF treated), $P < 0.05$; Fig. 2]. VEGF (2.0 nmol/L or 0.2 nmol/L) did not alter the invasion capacity of MDA-MB-231 (10 ± 8.0 cells). Addition of peptide BP1 resulted in a 50% decrease in PIGF-stimulated invasion (15 ± 4.2 cells; $P < 0.02$ versus PIGF only). The control peptide CPA did not inhibit the activity of PIGF (35 ± 17.3 cells). Addition of

anti-PIGF antibody (0.6 $\mu\text{g}/\text{mL}$) to the 0.2 nmol/L PIGF assays resulted in a 46% reduction in invasive cells (15 ± 2.3 cells). Taken together, these results suggest that PIGF stimulates invasiveness in the aggressive tumor cell line MDA-MB-231 and that the inhibitory peptide BP1, similar to the PIGF antibody, inhibits this activity. Similar results were obtained for MDA-MB-468 and MCF-7 but were not statistically significant (Table 3).

To test the therapeutic activity of the peptide BP1, mice were implanted with the human breast cancer cell MDA-MB-231, which produces lung metastases spontaneously

Table 2. PIGF-stimulated tumor cell motility inhibition by peptide BP1, Flt-1, anti-PIGF antibody, and anti-VEGF antibody

Cell line	Growth factor (2 nmol/L)	Test agent	Migrating cells	Relative activity
MDA-MB-231	0	0	23.8 ± 6.5	
	PIGF	0	$42.0 \pm 13.3^*$	100
	PIGF	Flt-1	$19.1 \pm 8.0^\dagger$	45
	PIGF	BP1	$13.6 \pm 6.1^\dagger$	32
	PIGF	CPA	39.8 ± 10.6	106
	PIGF	anti-PIGF	$17.0 \pm 6^\dagger$	40
	PIGF	anti-VEGF	34.4 ± 12.6	82
	VEGF	0	11.1 ± 1.8	100
	VEGF	BP1	14.7 ± 2.1	132
	VEGF	CPA	13.4 ± 4.5	121
	VEGF	anti-VEGF	11.5 ± 2.3	104
	VEGF	anti-PIGF	13.8 ± 14.6	124
	MDA-MB-468	0	0	13.4 ± 9.1
PIGF		0	14.7 ± 9.8	100
PIGF		Flt-1	$7.8 \pm 5.9^\dagger$	53
PIGF		BP1	14.3 ± 8.1	97
PIGF		CPA	21.6 ± 6.1	147
PIGF		anti-PIGF	$7.6 \pm 5.7^\dagger$	52
VEGF		0	14.0 ± 11.3	100
VEGF		BP1	15.8 ± 9.5	113
VEGF		CPA	14.6 ± 8.0	104
VEGF		anti-VEGF	14.2 ± 11.5	101
MCF-7	0	0	12.2 ± 11.4	
	PIGF	0	$22.1 \pm 13.4^*$	100
	PIGF	Flt-1	$10.4 \pm 8.2^\dagger$	47
	PIGF	BP1	$10.2 \pm 7.8^\dagger$	45
	PIGF	anti-PIGF	$10.9 \pm 4.9^\dagger$	49
	VEGF	0	12.7 ± 4.1	100
	VEGF	BP1	12.9 ± 2.9	102
	VEGF	CPA	19.4 ± 8.9	111
	VEGF	anti-VEGF	12.9 ± 4.3	102

NOTE: PIGF, VEGF, and Flt-1 were each at 2 nmol/L, and peptide was 2 $\mu\text{mol}/\text{L}$. Antibody concentration was 1 $\mu\text{g}/\text{mL}$. Results are presented as average number of cells migrating into the wound \pm SD from five to ten $\times 100$ microscopic fields per treatment per experiment at 18 to 24 h. $n = 2-6$ experiments (see Materials and Methods). Values for antibody treatments were from separate experiments, which included all relevant controls. Relative activity was determined by dividing the average value for the treatments by the PIGF-only or VEGF-only values. Addition of control antibody, Ag8, had no effect on cellular migration with or without added growth factor, except for MDA-MB-231, where PIGF-mediated migration was slightly inhibited (14%, $P > 0.1$).

* $P < 0.01$ (ANOVA) compared with untreated control.

$^\dagger P < 0.05$ (ANOVA) compared with PIGF only.

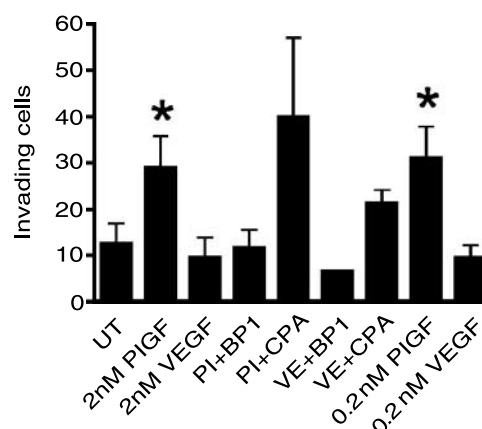


Figure 2. PIGF stimulates *in vitro* invasion of MDA-MB-231 cells. Cells were loaded into growth factor-depleted matrigel invasion chambers in 0.1% FBS-containing medium. Twenty-four hours after plating, cells on the upper sides of the wells were scraped off, the remaining cells stained with modified Wright's stain and counted at $\times 100$. Columns, cumulative results ($n = 2-5$ experiments); bars, SD. PI, PIGF; VE, VEGF; BP1, the active peptide; CPA, control peptide (see Materials and Methods); UT, cells without added peptide, growth factor, or serum. FBS-stimulated invasion was 62.8 ± 42.6 cells. *, $P < 0.05$ (ANOVA).

when implanted as s.c. tumor. When the tumors averaged $\sim 120 \text{ mm}^3$ in volume (see Materials and Methods), either mock treatment or therapy with BP1 was initiated at 200 μg at twice per week for 4 weeks ($n = 4$ mice per group). Mice receiving BP1 showed a 34% reduction in tumor size compared with mock-treated controls [tumor volumes: $689 \pm 559 \text{ mm}^3$ (mock treatment) versus $448 \pm 308 \text{ mm}^3$ (BP1 therapy)]. In a subsequent experiment, treatment was commenced when the tumors averaged 71 mm^3 ($n = 5$ mice per group). After 4 weeks of treatment, as described, the mean volumes of the mock-treated and CPA-treated tumors were $418 \pm 83 \text{ mm}^3$ and $332 \pm 271 \text{ mm}^3$, respectively, whereas, BP1-treated tumors averaged $56 \pm 23 \text{ mm}^3$ ($P < 0.05$ BP1-treated versus mock-treated or CPA-treated tumors; experiment 2; Fig. 3F).

Three to seven days after the final treatment, primary tumors and lungs were removed for microscopic examination (experiment 1 only, tissues from experiment 2 were not available for examination). Typically, the lungs of mock-treated animals contained multiple large and small metastases with many foci of tumor growth mostly surrounding the lung blood vessels spread into the surrounding parenchyma (Fig. 3B and C). The lungs of mock-treated controls averaged at 78 ± 25 nodules, 76 ± 19 clusters, and 36 ± 6 colonies per total lung tissue per mouse ($n = 4$ mice per group). In contrast, the BP1-treated lungs averaged 5 ± 2 nodules, 9 ± 2 clusters, and 5 ± 2 colonies per mouse ($n = 4$ mice per group; Fig. 3C). This constituted 94%, 88%, and 36% decreases in nodules, clusters, and colonies in the peptide-treated animals ($P < 0.007$ BP1 versus mock control).

In an orthotopic mammary fat pad model using MDA-MB-231, treatment with BP1 decreased tumor weight by 23% (mock treated, $0.423 \pm 0.089 \text{ g}$; CPA, $0.416 \pm 0.083 \text{ g}$;

Table 3. PIGF increases invasion potential of breast cancer cell lines

Cell lines	Untreated	PIGF	PIGF + BP1	PIGF + CPA	BP1
MCF-7	1.0	2.1 ± 0.7	0.3 ± 0.0	1.0 ± 0.6	0.7 ± 0.4
MDA-MB-231	1.0	4.4 ± 2.2*	1.3 ± 0.1 [†]	4.9 ± 2.4	1.0 ± 0.6
MDA-MB-468	1.0	1.8 ± 0.3	0.6 ± 0.4	1.2 ± 0.7	1.2 ± 0.3

NOTE: BP1 inhibits PIGF-mediated invasive potential. Average fold change in the number of cells on membranes after 24 h (MDA-MB-231) or 48 h (MDA-MB-468 and MCF-7) compared with untreated controls ± SD (concentration of serum, 0.1%; PIGF, 0.2 nmol/L; peptide, 2 µg/mL). *n* = 2–4 experiments per cell line. The average fold increase was calculated as the number of migrating cells in treated sample / the number migrating cells in untreated samples. Separate values for each experiment were averaged, and the SD was calculated. Untreated samples: 0.1% serum, no added growth factors or peptide. FBS stimulated increases of 3.2 ± 2.1-fold, 5.5 ± 1.9-fold, and 4.3 ± 2.7-fold for MCF-7, MDA-MB-231, and MDA-MB-468, respectively.

**P* < 0.01 versus untreated.

[†]*P* < 0.02 versus PIGF only.

BP1, 0.345 ± 0.095 g), which did not reach statistical significance. The mammary fat pad–implanted MDA-MB-231 did not produce large lung nodules, possibly due to the short duration of the experiment (4.5 weeks). However, micrometastases (20 to >100 cells) were apparently adjacent to pulmonary veins (Fig. 3D). These micrometastases numbered 3.4 ± 1.9, 2.8 ± 1.3, and 0.6 ± 0.5 per mouse for mock, CPA, and BP1 treatment (Fig. 3E), respectively (*P* < 0.02 versus mock or CPA treated), a reduction in metastases of 82%.

Similar treatment of mice (nude) bearing s.c. colon carcinoma, LoVo, which does not express PIGF or Flt-1 (11), had no effect on tumor growth (not shown).

Discussion

Several studies have documented that PIGF expression by cancers, including breast cancer, correlates with recurrence, metastasis, and mortality (4, 29–32). PIGF is also associated with a number of pathologic states (33) and tumor neovascularization (5, 21). Clinical studies of VEGF and PIGF in human cancer are conflicting. For instance, in one report, PIGF, rather than VEGF, stimulated growth of Philadelphia chromosome–positive acute myelogenous leukemias *ex vivo* (34). On the other hand, VEGF was associated with renal cell cancer stage, histologic grade, as well as its vascularity and venous invasion (35). These authors reported that PIGF was also an independent

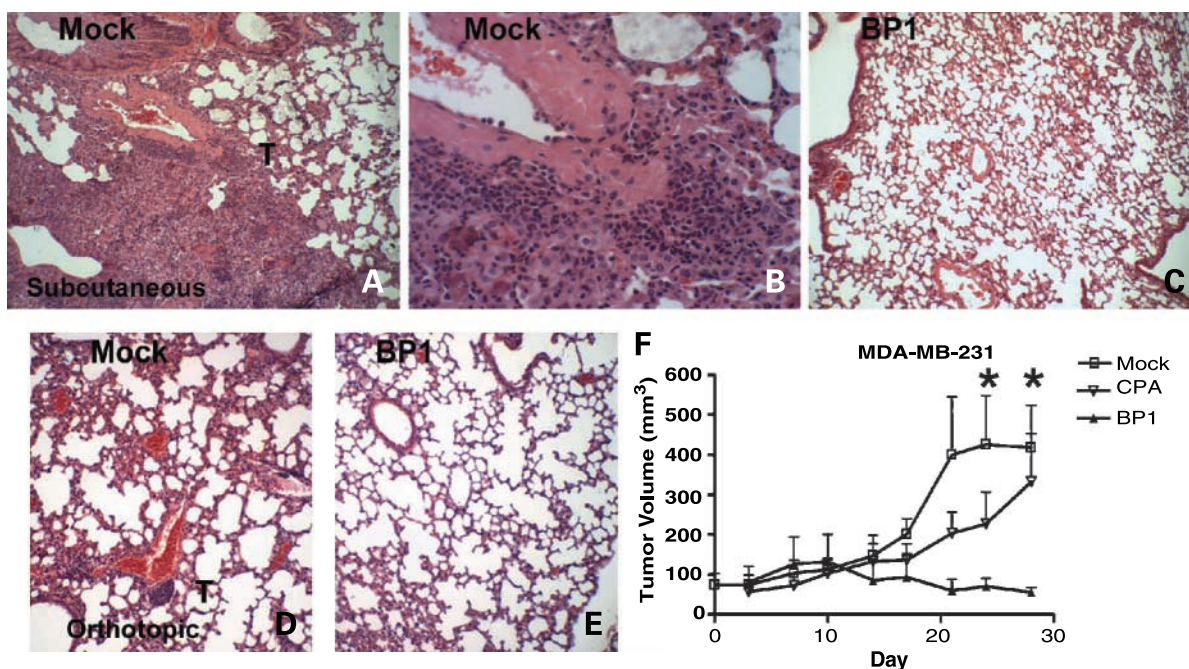


Figure 3. BP1 inhibits MDA-MB-231 xenograft growth and metastasis. **A** and **B**, metastases in the lungs of mock-treated mice in the s.c. xenograft model. **C**, BP1-treated lung (original magnification ×100). **D**, lung from mock-treated, orthotopic mammary fat pad model showing small metastasis. **E**, BP1-treated virtually tumor-free lung. (**A**, **C**–**E**, ×100; **B**, original magnification ×400). H&E stain. *T*, adjacent to tumor. **F**, tumor volume versus time, s.c. model. Points, results from one of two experiments (*n* = 3–4 mice per treatment); bars, SD. *, *P* < 0.05 versus mock treated or CPA treated (change in tumor volume, ANOVA).

prognostic factor for this cancer. Thus, the evidence from these studies of human cancers warrants investigating possible extraangiogenic functions for PIGF in breast cancer pathology.

The data presented in this study indicate that PIGF enhances the metastatic potential of breast cancer cells, because it stimulates motility and invasiveness, which are associated with the epithelial-to-mesenchymal transformation that characterizes metastasis in tumors. In contrast, exogenously added VEGF had no effect on tumor cell motility or invasiveness in these assays. These results differ from those of Bachelder et al. (36), where VEGF was found to be a stimulator of invasion (MDA-MB-231). However, this study did not include PIGF; therefore, comparisons of the growth factors cannot be made. Our results are based on the presence of PIGF or VEGF in the tumor cell environment, whereas Bachelder et al. (36) used RNAi to suppress VEGF production by the cells, the results of which may differ from VEGF paracrine effects. Another report documented an inhibitory role for PIGF when it is overexpressed by tumor lines that are normally low-PIGF, high-VEGF expressers (37). This pattern of expression differs from that of the breast lines used in the present study, which were high-PIGF, low-VEGF expressers, and which, therefore, mimic primary human breast carcinomas. At least one other study showed that VEGF and PIGF synergize to stimulate angiogenesis in pathologic conditions (33). The contribution of PIGF or VEGF to tumor pathology is most likely complex and may in part be due to their relative abundance in the tumor microenvironment, as well as the presence of their active receptors on tumor cells and endothelium. In the present study, the capacity of PIGF to stimulate cancer cell motility and invasion was inhibited with anti-PIGF antibody, as well as with BP1, the PIGF-2/Flt-1 antagonistic peptide we developed. It could be surmised that if PIGF were inhibitory, then its removal would allow VEGF-mediated activity to proceed, which was not the case.

To elucidate the role of PIGF in tumor and endothelial cell biology, we developed an antagonistic peptide, BP1, which inhibited the activity of PIGF on both tumor and endothelial cells and affected spontaneous metastasis *in vivo*. The results herein indicate that BP1 antagonizes PIGF-2/Flt-1 heparin associations. Heparin-binding is essential for the full activation of some receptor tyrosine kinases (17, 18, 38). By preventing the close association of heparin with PIGF-2 and Flt-1, BP1 may prevent the transmission of activation signals to the interior of the cell. We appreciate, however, that more studies are needed to further define the mechanism of action of this peptide.

While this work was being completed, Bae et al. (39) reported the anticancer potential of a Flt-1 antagonistic peptide that inhibited VEGF binding to Flt-1, as well as the growth and metastasis of VEGF-secreting colon tumor xenografts. The activity of this peptide was determined by its interaction with endothelial cells using VEGF as the stimulator of migration and proliferation rather than tumor cells. It is interesting that the peptide used by these authors

also inhibited the binding of PIGF to Flt-1, and part of its efficacy may stem from this interaction. Their peptide, however, seems to differ from BP1, because it interferes with the Flt-1 domain 2 growth factor binding site (39), with no evidence of interaction with the heparin-binding domain. Thus, the peptide presented by Bae et al. most likely functions differently from BP1.

The *in vivo* role of PIGF in cancer was studied by treating human breast cancer xenografts that metastasize spontaneously with BP1. Treatment with the peptide BP1 arrested s.c. MDA-MB-231 tumor growth and decreased the occurrence of pulmonary metastases by ~90%, and by 82% in an orthotopic mammary fat pad model. It is possible that the effects on pulmonary metastases were indirect and due to inhibition of tumor cell growth rather than ablation of the metastatic phenotype. This question needs to be clarified with further experimentation. Although the *in vivo* activity of these peptides has not been fully characterized, the *in vitro* data suggest antagonism of Flt-1 activity and that this receptor may play a key role in the progression of certain cancers, perhaps representing a target for anticancer therapy.

In summary, these studies expand our knowledge of the role of PIGF in malignancy by demonstrating (a) its expression in both primary human breast cancers and cell lines, (b) that exogenous PIGF increases migration and invasion of breast cancer cells *in vitro*, (c) that the antagonistic Flt-1-BP1 inhibits tumor cell motility and invasive potential, and (d) that this peptide inhibits tumor growth and metastasis *in vivo*. To our knowledge, this is the first report documenting the direct activation of malignant cells by PIGF and the blocking of certain PIGF-2/Flt-1 functions, including metastasis, by an antagonistic peptide that interferes with heparin binding.

Acknowledgments

We thank Marisol Hernandez, Marisol Rodriguez, Evelyn Leon, and Nino Velasco for technical assistance with histology, flow cytometry, and animal care, and Gopi Patel for tumor measurements.

References

1. Lical PM, Failla CM, Pagani E, et al. Human melanoma cells secrete and respond to placenta growth factor and vascular endothelial growth factor. *J Invest Dermatol* 2000;115:1000–7.
2. Cao Y, O'Reilly MS, Marshall B, Flynn E, Richard-Weidong J, Folkman J. Expression of angiostatin cDNA in a murine fibrosarcoma suppresses primary tumor growth and produces long-term dormancy of metastases. *J Clin Invest* 1998;101:1055–63.
3. Donnini S, Machein MR, Plate KH, Weich HA. Expression and localization of placenta growth factor and PIGF receptors in human meningiomas. *J Pathol* 1999;189:66–71.
4. Wei S-C, Tsao P-N, Yu S-C, et al. Placenta growth factor expression is correlated with survival of patients with colorectal cancer. *Gut* 2005;54:666–72.
5. Li B, Sharpe EE, Maupin AB, et al. VEGF and PIGF promote adult vasculogenesis by enhancing EPC recruitment and vessel formation at the site of tumor neovascularization. *FASEB J* 2005;20:1495–7.
6. Maglione D, Guerriero V, Viglietto G, et al. Isolation of a human placenta cDNA coding for a protein related to the vascular permeability factor. *Proc Natl Acad Sci U S A* 1991;88:9267–71.
7. Viglietto G, Maglione D, Rambaldi M, et al. Upregulation of vascular endothelial growth factor (VEGF) and downregulation of placenta growth

- factor (PIGF) associated with malignancy in human thyroid tumors and cell lines. *Oncogene* 1995;11:1569–79.
8. Failla CM, Odorisio T, Cianfarani F, Schietroma C, Puddu P, Zambruno C. Placenta growth factor is induced in human keratinocytes during wound healing. *J Invest Dermatol* 2000;115:388–95.
 9. Gleadle JM, Ebert BL, Firth JD, Ratcliffe PJ. Regulation of angiogenic growth factor expression by hypoxia, transition metals, and chelating agents. *Am J Physiol* 1995;268:C1362–8.
 10. Yonekura H, Sakurai S, Liu X, et al. Placenta growth factor and vascular endothelial growth factor B and C expression in microvascular endothelial cells and pericytes. Implication in autocrine and paracrine regulation of angiogenesis. *J Biol Chem* 1999;274:35172–8.
 11. Taylor AP, Osorio L, Craig R, Ying Y, Goldenberg DM, Blumenthal RD. Tumor-specific regulation of angiogenic growth factors and their receptors during recovery from cytotoxic therapy. *Clin Cancer Res* 2002;8:1213–22.
 12. Green CJ, Lickten P, Huynh NT, et al. Placenta growth factor gene expression is induced by hypoxia in fibroblasts: a central role for metal transcription factor-1. *Cancer Res* 2001;61:2696–703.
 13. Luttun A, Tjwa M, Moons L, et al. Revascularization of ischemic tissues by PIGF treatment, and inhibition of tumor angiogenesis, arthritis and atherosclerosis by anti-Flt-1. *Nat Med* 2002;8:831–40.
 14. Migdala M, Huppertz B, Tessler S, et al. Neuropilin-1 is a placenta growth factor-2 receptor. *J Biol Chem* 1998;273:22272–8.
 15. Hauser S, Weich H. A heparin-binding form of placenta growth factor (PIGF-2) is expressed in human umbilical vein endothelial cells and in placenta. *Growth Factors* 1993;9:259–68.
 16. Neufeld G, Kessler O, Herzog Y. The interaction of neuropilin-1 and neuropilin-2 with tyrosine-kinase receptors for VEGF. *Adv Exp Med Biol* 2002;515:81–90.
 17. Park M, Lee ST. The fourth immunoglobulin-like loop in the extracellular domain of Flt-1, a VEGF receptor, includes a major heparin-binding site. *Biochem Biophys Res Commun* 1999;264:730–4.
 18. Schlessinger J, Plotnikov AN, Ibrahim OA, et al. Crystal structure of a ternary FGF-FGFR-heparin complex reveals a dual role for heparin in FGFR binding and dimerization. *Mol Cell* 2000;6:743–50.
 19. Soker S, Fidler IJ, Neufeld G, Klagsbrun M. 1996. Characterization of novel vascular endothelial growth factor (VEGF) receptors on tumor cells that bind VEGF165 via its exon 7-encoded domain. *J Biol Chem* 1996;271:5761–7.
 20. Errico M, Riccioni T, Iyer S, et al. Identification of placenta growth factor determinants for binding and activation of the flt-1 receptor. *J Biol Chem* 2004;279:43929–39.
 21. Taylor AP, Rodriguez M, Adams K, Goldenberg DM, Blumenthal RD. Altered tumor vessel maturation and proliferation after radioimmunotherapy: Potential relationship to post-therapy tumor angiogenesis and recurrence. *Int J Cancer* 2003;105:158–69.
 22. Adini A, Kornaga T, Firoozbakht F, Benjamin LE. Placental growth factor is a survival factor for tumor endothelial cells and macrophages. *Cancer Res* 2002;62:2749–52.
 23. Prickett KS, Amberg DC, Hopp TP. A calcium-dependent antibody for identification and purification of recombinant proteins. *BioTechniques* 1989;7:580–9.
 24. Castrucci MR, Bilsel P, Kawaoka Y. Attenuation of influenza A virus by insertion of a foreign epitope into the neuraminidase. *J Virol* 1992;66:4647–53.
 25. Verma A, Davis GE, Ihler GM. Formation of stress fibres in human endothelial cells infected with *Bartonella bacilliformis* is associated with altered morphology, impaired migration and defects in cell morphogenesis. *Cell Microbiol* 2001;3:169–80.
 26. Sung Y-J, Sung Z, Ho C-L, et al. Intercellular calcium waves mediate preferential cell growth toward the wound edge in polarized hepatic cells. *Exp Cell Res* 2003;287:209–18.
 27. Itokawa T, Nokihara H, Nishioka Y, et al. Antiangiogenic effect by SU5416 is partly attributable to inhibition of flt-1 receptor signaling. *Mol Cancer Ther* 2002;1:295–302.
 28. Kuperwasser C, Dessain S, Bierbaum BE, et al. A mouse model of human breast cancer metastasis to human bone. *Cancer Res* 2005;65:6130–8.
 29. Chen CN, Hsieh FJ, Cheng YM, et al. The significance of placenta growth factor in angiogenesis and clinical outcome of human gastric cancer. *Cancer Lett* 2004;213:73–82.
 30. Parr C, Watkins G, Boulton M, Cai J, Jiang WG. Placenta growth factor is over-expressed and has prognostic value in human breast cancer. *Eur J Cancer* 2005;41:2819–27.
 31. Weidner N, Carroll PR, Flax J, Blumenfeld W, Folkman J. Tumor angiogenesis correlates with metastasis in invasive prostate carcinoma. *Am J Pathol* 1993;143:401–9.
 32. Zhang L, Chen J, Ke Y, Mansel RE, Jiang WG. Expression of Placenta growth factor (PIGF) in non-small cell lung cancer (NSCLC) and the clinical and prognostic significance. *World J Surg Oncol* 2005;3:68.
 33. Carmeliet P, Moons L, Luttun A, et al. Synergism between vascular endothelial growth factor and placental growth factor contributes to angiogenesis and plasma extravasation in pathological conditions. *Nat Med* 2001;7:575–83.
 34. Ikai T, Miwa H, Shikami M, et al. Placenta growth factor stimulates the growth of Philadelphia chromosome positive acute lymphoblastic leukemia cells by both autocrine and paracrine pathways. *Eur J Haematol* 2005;75:273–9.
 35. Matsumoto K, Suzuki K, Koike H, et al. Prognostic significance of plasma placental growth factor levels in renal cell cancer: an association with clinical characteristics and vascular endothelial growth factor levels. *Anticancer Res* 2003;23:4953–8.
 36. Bachelder R, Wendt M, Mercurio A. Vascular endothelial growth factor promotes breast carcinoma invasion in an autocrine manner by regulating the chemokine receptor CXCR4. *Cancer Res* 2002;62:7203–6.
 37. Xu L, Cochran DM, Tong RT, et al. Placenta growth factor overexpression inhibits tumor growth, angiogenesis, and metastasis by depleting vascular endothelial growth factor homodimers in orthotopic mouse models. *Cancer Res* 2006;66:3971–7.
 38. Ito N, Claesson-Welsh L. Dual effects of heparin on VEGF binding to VEGF receptor-1 and transduction of biological responses. *Angiogenesis* 1999;3:159–66.
 39. Bae D-G, Kim T-D, Li G, Yoon W-H, Chae C-B. Anti-flt1 peptide, a vascular endothelial growth factor receptor 1-specific hexapeptide, inhibits tumor growth and metastasis. *Clin Cancer Res* 2005;11:2651–61.